Available online at www.sciencedirect.com

SciVerse ScienceDirect

Journal of the European Ceramic Society 32 (2012) 1137–1147

www.elsevier.com/locate/jeurceramsoc

Thermodynamic approach to the vaporization and growth phenomena of SiC ceramics. II. The SiC surface under oxidative conditions

G. Honstein, C. Chatillon *, F. Baillet

Science et Ingénierie des Matériaux et Procédés (SIMAP associé au CNRS-UMR 5466, UJF/INP-Grenoble), Domaine Universitaire, BP 75, 38402 Saint Martin d'Hères, France

Available online 17 December 2011

Abstract

Thermodynamic conditions at the SiC surface under oxygen pressure are analyzed from two points of view: (i) the conditions for creation of a first layer of silica and (ii) the conditions for carbon precipitation. The active to passive oxidation transition steady-state is studied using a thermodynamic analysis focused on the chemical potential of silicon and oxygen at the surface of the compound in order to ensure the existence of a clean SiC surface, *i.e.* a flow balance imposed simultaneously for the Si and C vaporization flows Si/C = 1/1 at the surface. Thermodynamic calculations show that there exists a window in the couple as a function of temperature that corresponds to a bare SiC surface. For such prevailing conditions the SiC erosion flows are calculated as well as the related SiC condensation phenomenon that might explain the SiC transport and vapor phase deposition at high temperature.

Keywords: Thermodynamics; SiC; Active oxidation; Growth

1. Introduction

SiC as many Si based compounds, is relatively stable in oxidizing atmospheres because of the formation of a SiO_2 layer on its surface. Certain oxidative conditions are needed to form this layer that corresponds to the so-called "passive oxidation" conditions. If these conditions are not fulfilled, *i.e.* the oxygen pressure decreased below a certain limit, the SiO_2 layer will be eliminated for example by vaporization of SiO(g) and CO(g) in vacuum or in a carrier gas. Then the incident oxygen flow on the SiC surface becomes instantaneously balanced by the vaporization flow of CO(g) and SiO(g) and SiC presents a surface free from silica that will be eroded continuously by the incident oxygen flow according roughly to the main reaction,

$$\mathrm{SiC(s)} + \mathrm{O_2(g)} = \mathrm{SiO(g)} + \mathrm{CO(g)}$$
$$\text{with} \quad K_p(T) = \frac{p_{\mathrm{SiO}} \cdot p_{\mathrm{CO}}}{a_{\mathrm{SiC}} \cdot p_{\mathrm{O_2}}} \tag{1}$$

In this case the oxidation is called "active oxidation" and the SiC mass loss or erosion rate becomes different from the one for passive oxidation when SiC is covered by a SiO_2 layer. Note that according to the equilibrium constant of reaction (1) if the Si/C atomic ratio of the evaporating gas phase is equal to 1 – *i.e.* equal to the bulk SiC composition ratio – the surface of SiC remains free from any precipitation as for instance carbon by excess of SiO(g) vaporization or silicon by excess of CO(g) vaporization. Between the two oxidation regimes there exist a transition "active to passive" or reversely. According to the literature, this transition has been studied experimentally and theoretically depending on the way the oxygen flow arrives at the surface, on the flow departure of reaction products, on temperature and finally on the nature and structure of the SiC material. The present work is focused: (i) on the way to define the SiC surface thermodynamic conditions that warranty the existence of a "bare" or clean SiC surface in order to favor any growth process, (ii) on an exact approach of the active to passive transition from the point of view of the SiC surface chemical potentials.

2. Brief literature survey on active oxidation of SiC and transition active-to-passive

2.1. Experimental works

Experimental and theoretical first studies of the so-called "active-to-passive transition" have been summarized in 1990

* Corresponding author. Tel.: +33 0476 82 65 11; fax: +33 0476 82 67 67.
E-mail address: christian.chatillon@simap.inp-grenoble.fr (C. Chatillon).

0955-2219/$ – see front matter © 2011 Elsevier Ltd. All rights reserved.
doi:10.1016/j.jeurceramsoc.2011.11.031

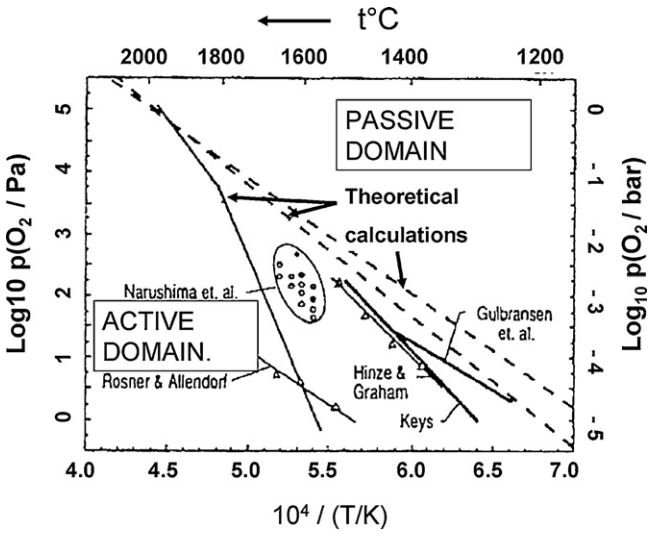

Fig. 1. Summary of active-to-passive transition from experimental and theoretical works as presented by Vaughn and Mass[1] in 1990. The mentioned pressures are the partial pressure of oxygen in the flowing gas at the entrance in the furnace.

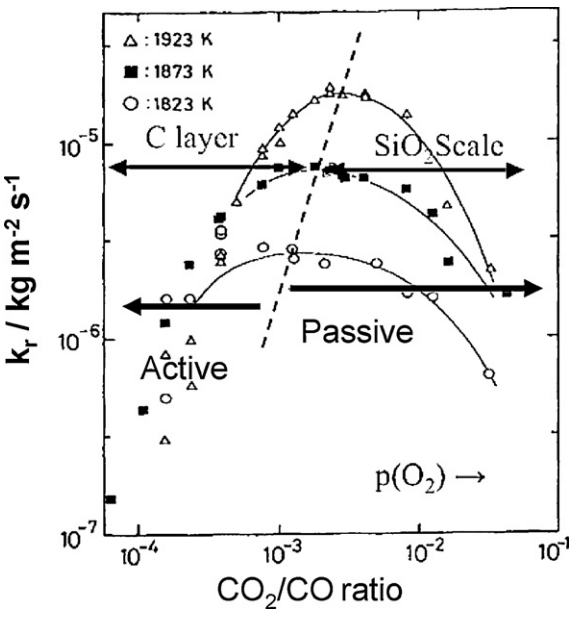

Fig. 2. Example of TGA experimental work as performed by Narushima et al.[3] in order to study the active-to-passive transition. The transition is proposed by the authors to occur at the maximum rate. The CO_2/CO ratio is the one in the flowing gas at the furnace entrance. K_r is the erosion rate constant.

by Vaughn and Mass[1] as shown in Fig. 1 according to a diagram $\{\log p(O_2), 1/T(K)\}$. The oxygen pressure is the one in the gas flow at the entrance of the furnace (cold side). Variations in the experimental collected data – and especially for the active to passive transition – are attributed by the authors to the nature of the SiC material (hot pressed, sintered, CVD deposition, etc.) and to the wide range of pressures, of flow rates and oxidizing gas mixtures compositions.

Experimental observation of the transition active to passive is usually performed using thermogravimetric analysis (TGA) because the passive regime is associated with a net mass increase due to the build up of the SiO_2 layer under an imposed gas flow. The oxygen partial pressure mentioned on the *y*-axis (in Fig. 1) is the one existing in the flowing gas often diluted in neutral gas at a fixed total pressure of 1 atm, although lower pressures were also used. One suggestion made by Hinze and Graham[2] is that the transition pressure is determined and controlled by the CO(g) out-flow from the SiC surface.

Later, Narushima et al.,[3] investigated by TGA the oxidation behavior of CVD-SiC (obtained by chemical vapor deposition) under CO/CO_2 flows in the 1823–1923 K range. They observed linear mass loss behavior with time meaning that the oxidation corresponds to a steady-state, the rate constant being maximal for a certain CO/CO_2 ratio as presented in Fig. 2. For lower values of this ratio the authors observed after experiment a carbon layer at the surface, meanwhile at higher values a silica (cristobalite) layer. The maximum of the rate constant is attributed by the authors to the active-to-passive transition. Opila and Hann[4] using TGA under H_2O/O_2 flow in the 1472–1673 K range observed also a paralinear oxidation rate for CVD-SiC in the passive domain. This behavior is attributed to the volatilization of the silica layer by silanols ($Si(OH)_4$, $Si(OH)_2$, SiO(OH), etc.). Schneider et al.,[5] by TGA in the 1573–1973 K range with SiC square plates submitted to a parallel gas flow at low pressures (100–800 Pa) and high velocity, observed at constant velocity an increase of the mass loss followed by a decrease when increasing oxygen pressure in the input gas flow. The maximum is attributed to the transition as told by Narushima et al. meanwhile a silica layer is observed after the experiments. In the high temperature domain (≥1900 K) the maximum is not observed as well as the silica layer meaning that the oxygen arrival is too weak to undergo the transition from active to passive.

The SiC oxidation has been also studied using molecular or atomic oxygen in relation with aerospace applications. Dealing with earlier works, Rosner and Allendorf[6] observed the cross section variations of a SiC tore (deposited around a W heating wire) submitted to a $\{Ar + O_2(g)$ or $O(g)\}$ flow at low total pressure (1 Torr, *i.e.* 133 Pa) as a function of temperature (1750–2400 K) and oxygen concentration. The SiC removal rate constant–thus corresponding to the active oxidation – for the two $O_2(g)$ and O(g) species were not very different, but the observed active-to-passive transition at the same temperature differed by a factor 100 to 10 for the oxygen pressure when going from low to high temperatures. For the same temperature, passive oxidation occurred at higher pressures for $O_2(g)$ and the difference decreased with temperature. This feature let suppose that the $O_2(g)$ decomposition at the surface into adsorbed atomic O on favorable sites (O_{ads}) and further reaction to form CO(g) and SiO(g) is a limiting step or that some O_2 molecules are lost by partial desorption (or reflection) during the thermal accomodation in the physisorbtion first step – *i.e.* the collision with the surface.

Balat et al.,[7] used a special laminar flow apparatus with $\{$neutral gas + $O_2(g)$ or $O(g)\}$ in the 1653–1948 K range with pressures in the 200–2100 Pa range. After experiments, the SiC mass gain is measured and the SiC surface layers were analyzed by XRD for thick layers and by Auger Spectroscopy for thin layers. The transition with $O_2(g)$ occurred at slightly lower

temperatures than with O(g) in the same conditions, meaning that the oxidation is easier with O_2(g). This feature disagrees with the observations of Rosner and Allendorf[6] and seems strange because the impinging of a surface with a molecule involves usually an intermediate step for decomposition before adsorption of the atoms and this phenomenon should "hinder" (or "retard") the reactions at the surface or eliminate some O_2 molecules before adsorption – a necessary step for further surface reactions except if the direct adsorption of the molecule O_2 is favorable. But yet the observed difference could be explained by the large uncertainty (±50 to 60 K) associated with the knowledge of the surface temperature or by the difficulties to quantify exactly the O content that arrive from the plasma source at the SiC surface due to uncontrolled re-combinations into O_2(g).

2.2. Theoretical works

Some theoretical works are directly related to the interpretation of the experimental results by their authors, others are independent calculations. Some interpretations are based on the earlier work of Wagner[8] for the active to passive oxidation of silicon in a viscous gas flow. At high pressures, silica could be formed either as a scale at the surface of the SiC or as a cloud in front of the SiC surface ("smoke cloud"). The flow of incident oxygen and those of the escaping products (SiO(g) and CO(g) – the only species taken into account in these studies – are controlled by gas diffusion in a boundary layer). Assumptions are necessary to quantify the diffusion flows: (i) the composition in the gas flow introduced was assumed constant beyond the diffusion layer due to convection or laminar flow and corresponded for oxygen to the introduced steady-state quantity, (ii) the thickness of the boundary layer, (iii) the knowledge of the chemical potential at the interface SiC/SiO_2. This last one is generally taken–see for instance Hinze and Graham[2] – as the one for the congruent reaction,

$$\mathrm{SiC(s)} + 2\,\mathrm{SiO_2(s)} = 3\,\mathrm{SiO(g)} + \mathrm{CO(g)}$$

$$\text{with} \quad K_p(T) = \frac{p_{\mathrm{SiO}}^3 \cdot p_{\mathrm{CO}}}{a_{\mathrm{SiC}} \cdot a_{\mathrm{SiO_2}}^2} \tag{2}$$

with the activities of the solids equal to 1, and the pressure ratio $p_{SiO}/p_{CO} = 3/1$, *i.e.* the congruent condition for vaporization that correspond to a fixed value of the oxygen potential. Diffusion coefficients in the neutral gas are included in the flow ratio to compute the transition. In case of lower pressures the diffusion boundary layer is vanishing and the oxygen introduced is really the one arriving at the surface. Consequently comparing different experiments according to Fig. 1, the real steady-state oxygen pressure at the surface of the SiC will be lower than the introduced one's as mentioned along the *y*-axis when the total pressure increases. This is one of the possible explanations for scattered experimental results in Fig. 1.

As recently summarized by Opila and Jacobson,[9] two other different main reactions have been chosen as assumptions at the interface SiC/SiO_2

$$\mathrm{SiC(s)} + \mathrm{SiO_2(s)} = 2\,\mathrm{SiO(g)} + \mathrm{C(s)},$$

i.e. the triphasic SiC–SiO_2–C vaporization (3)

$$2\,\mathrm{SiC(s)} + \mathrm{SiO_2(s)} = 3\,\mathrm{Si(s)} + 2\,\mathrm{CO(g)},$$

i.e. the triphasic Si–SiC–SiO_2 vaporization. (4)

We observe that reactions (2)–(4) assume that the activity of Si (or C) at the interface SiC/SiO_2 can vary from one diphasic SiC–Si to the other SiC–C. Taking into account on the diffusion layer in the gas phase close to the SiC surface, relations between the O_2(g) transition pressure in the bulk gas phase and one main gaseous species created at the interface (SiO(g) generally) are obtained in the form,

$$p_{\mathrm{O_2}}^{\mathrm{transition}} = \left[\frac{D_{\mathrm{SiO}}}{D_{\mathrm{O_2}}}\right]^{1/2} p_{\mathrm{SiO}}^{\mathrm{eq}} \tag{5}$$

with reaction (3) for instance. All these calculations would be available for laminar or viscous flows but no available experimental checks have been done to certify the real interface reaction state at the creation of the first silica layer in the whole range of available Si activities compatible with the existence of the SiC compound.

The volatility diagrams as presented by Heuer and Lou[10] present the partial pressures of the main species as a function of the oxygen one (or another variable like the CO/CO_2 or H_2O/O_2 ratios) for different fixed CO(g) pressures and with the different combinations of stable condensed phases. Sometimes, a CO(g) partial pressure diagram is also superimposed to this diagram. In the case of the Si–C–O system the lines may be the partial pressures of mainly SiO(g) and Si(g) or SiO_2(g) species as a function of oxygen pressures for different diphasics as for instance SiC–C or SiO_2–C and their intersection points are for the triphasics as Si–SiC–SiO_2 and SiC–SiO_2–C. In this system SiO(g) is altogether with CO(g) very often the main species as presented for instance in Fig. 3. In case of triphasics, the variance equals 0 when temperature is fixed and the pressures are imposed by the set of condensed phases. Additionally, when the variance becomes equal to 1 as for the diphasics a

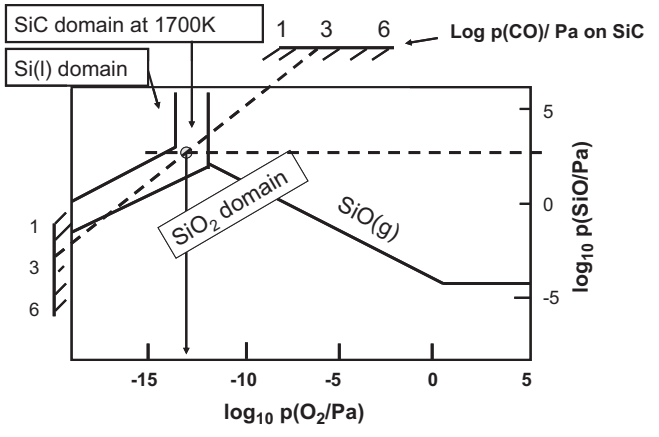

Fig. 3. Example of volatility diagram at 1700 K for the system Si–C–O: values from Heuer and Lou.[10] An example of equal pressures for CO(g) and SiO(g) – doted lines as representing the ratio 1/1 for active oxidation – is presented with the intersection in the SiC existence domain at 1700 K.

supplementary condition could be imposed as for instance: (i) some constant partial pressure in order to find the condensed phase in equilibrium with or, (ii) some pressure ratios as for instance the one SiO/CO = 1/1 for active oxidation as we have done in Fig. 3. But yet the intersection of the partial pressures of CO and SiO (at the same value) in the SiC existence domain corresponding to this ratio cannot really represent the active oxidation of SiC since the variance becomes equal to -1 due to a total pressure (mainly $p(CO) + p(SiO)$) also fixed at the same time the present ratio would be fixed. Indeed, in the course of the present work we observed that the pressure of oxygen from Fig. 3 is far above the calculated one for active oxidation at 1700 K due to a total pressure SiO(g) + CO(g) too high. Any other reasoning as done by the authors about the "silica smoke" and the "blow out" of this cloud and its possibility to join the surface to start the passive oxidation is speculative since these mechanisms would be relevant of only flow calculations associated with thermodynamic constraints well localized (at the surface or in a smoke cloud).

The approach of Nickel et al.,[11] was to perform thermodynamic calculations in a configuration that can be related to some particular experimental or practical situations. As thermodynamics needs well defined variables, the authors use temperature and total pressure constants and a number of moles of SiC with a fixed number of moles of the partial pressure H_2O/H_2 ratio, *i.e.* the oxygen potential in the introduced gas quantity. The conversion of part of the oxygen introduced in the flow into different gaseous species by thermodynamics leads to the consumption of SiC for a fixed exchange rate, *i.e.* relative gas flow moles to SiC moles. At a fixed flow of gas and constant SiC moles, the sequences of stable condensed phases when increasing temperature is SiO_2–SiC–C, SiO_2–SiC, SiC, SiC–Si and finally Si at very high temperature since SiO(g) and CO(g) proportions increase with temperature. Theoretical passive-to-active boundary is thus defined during a temperature increase when SiO_2 disappears. Their Fig. II.14.3 presents a line for this transition as a function of the introduced oxygen potential (H_2O/H_2 ratio) which is not the one at the surface of SiC after reaction, *i.e.* the oxygen potential surface steady-state, but is dependent on the exchange rate (not mentioned). Additionally we observe in their Fig. II-14.2 a temperature range for the existence of pure SiC between the disappearance of SiO_2 (SiO_2–SiC phases) and the appearance of Si (SiC–Si phases). We shall see in the present work that this range corresponds to silicon activities (or C activities) within the stoichiometric domain of the pure compound SiC. In order to calculate corrosion rates (in mm/year/surface) Nickel et al.,[11] calculated the related flow of matter loss using the Hertz–Knudsen flow which is the maximum available evaporated flow (equilibrium) corresponding to the total sweep out of the gas issued from the surface of SiC by a high velocity flowing gas. As the gas phase escaping from the surface of SiC is calculated with the so imposed oxygen potential, the SiO(g)/CO(g) active ratio equal to 1/1 is not taken into account as a constraint but is only the result of the conversion of the oxygen from H_2O(g) into {SiO(g) + CO(g)} at equilibrium that normally should produce different ratios SiO/CO depending on initial conditions and temperature. But yet, in their Figs. II.14.2.(a) and (b) this ratio seems to tend to the active oxidation 1/1 value in the SiC existence domain. We shall see in the present work that this condition is automatically fulfilled for a certain silicon activity range. In their final calculations of corrosion rates, the authors showed in their Fig. II.14.4. an active oxidation domain between pure Ar flow and the precipitation of SiO_2 (passivation), whatever is the water content. In their calculations they observed the precipitation of carbon that influence the corrosion rate, but no indications are reported on the figure for this domain and the carbon precipitation is considered included in the active oxidation domain.

3. SiC behavior under active oxidation

Considering molecular regime (Knudsen regime) as the predominant vaporization process, *i.e.* the maximum vaporization flow available at the surface, and all elementary reactions between the solid components for gases creation, we can calculate the limits of oxygen partial pressure at the reacting surface for pure SiC. The reacting surface of pure SiC can precipitate either carbon or begin to form a SiO_2 layer. Thus, we are looking for the limits of oxygen partial pressures at the SiC surface which allows to keep the SiC surface bare or "clean", *i.e.* without any matter precipitation in order to favor growth processes. Following, we have to consider two transition limits: active-to-passive (SiO_2 formation) and carbon precipitation.

3.1. Limits of active oxidation of SiC

For the calculation of oxygen partial pressure steady-state at the limit of carbon precipitation we first calculate the silicon activity corresponding to carbon activity = 1 for the phase limit SiC–C. By varying the steady-state oxygen pressure $p(O_2)$ at the surface, the Si and C atomic flows escaping from the surface–with a formalism already presented by Honstein et al.,[12] in part I – are compared until to their ratio F_{Si}/F_C be equal to 1. As the maximum $p(O_2)$ which corresponds to the three-phases domain SiO_2–SiC–C induces an atomic flow ratio $F_{Si}/F_C < 1$, from this maximum value, $p(O_2)$ is then decreased until the ratio $F_{Si}/F_C = 1$ is found. We performed this calculation for each temperature in the concerning temperature range.

For the other limit – creation of a SiO_2 layer – the already calculated congruent vaporization of SiC–SiO_2 interface is a particular case of SiC/SiO_2 interface reaction with the partial pressures ratio of SiO(g) to CO(g) being equal to 3 (viscous flow) or 3.76 (Knudsen flow) according to the main vaporization reaction (2) as already discussed in part I.[12] The congruent vaporization in fact corresponds to a particular chemical state of the interface SiC/SiO_2 – *i.e.* a couple of parameters $\{p(O_2), a_{Si}\}$ – and does not correspond to the other limit described above, *i.e.* the onset of SiO_2 precipitation with the C/Si evaporation flow ratio equal to 1 in place of 3 (or 3.76). This active oxidation limit is thus located at a different $\{p(O_2), a_{Si}\}$ couple of variables since the Si and C flow conditions for a bare SiC surface are definitely different from the one corresponding to the congruent interface SiO_2–SiC.

Trying to find the limit of SiO_2 precipitation we made an attempt starting at very low $p(O_2)$ which corresponds to the limit SiC–C active oxidation as calculated above and varying a(Si) in the SiC existence domain by increasing steps and then increasing the oxygen pressure and retaining the $p(O_2)$ value which would produce $F_{Si}/F_C = 1$. Calculations are close to the rough condition $p_{SiO}/p_{CO} = 1$ due to the main reaction (1). Nevertheless, depending on temperature and due to the numerous gaseous species involved in the vaporization processes (see part I), the thru atomic flow ratio F_{Si}/F_C is always calculated taking into account of all gaseous species.

For a_{Si} increasing close to 1 we could not find any solution because for instance at the limit Si–SiO_2 the SiO(g) partial pressure (corresponding also to the triphasic Si–SiO_2–SiC) is always much higher than p(CO) as shown for instance by Rocabois et al.,[13] and calculated in part I paper.[12] Thus the solution for calculating the available oxygen pressure of active oxidation can only be found when beginning from low a_{Si} (SiC–C limit), increasing step by step this activity, scanning by increasing amounts the oxygen pressure and stopping at maximum $p(O_2)$ that corresponds to SiO_2 formation according to the reaction

$$Si(s, s) + O_2(g) = SiO_2(s) \quad \text{with} \quad K_p = \frac{a_{SiO_2}}{a_{Si} \cdot p_{O_2}} \tag{6}$$

The SiO_2 activity is 1 and $p(O_2)$ is depending on the silicon activity which is chosen within the SiC compound existence domain. This oxygen pressure is the active oxidation limit at the silica layer creation for a certain silicon activity. Practically, for each set of a_{Si}, varying from its minimum at the SiC–C limit up to 1, at constant temperature we scanned the oxygen partial pressure and then the flow ratio F_{Si}/F_C. Close to the phase limit Si–SiC ($a_{Si} \to 1$) this ratio was always >1 and no solution was found. As long as the flow ratio F_{Si}/F_C could be found equal to 1 for a certain fixed a_{Si}* when varying $p(O_2)$ the condition of active oxidation exists. At that time we found the couple of conditions $\{a_{Si}^*, p(O_2)^*\}$ which corresponds to the creation of the first SiO_2 layer according to the above equilibrium (6). The final limit is determined when no couples $\{a_{Si}^*, p(O_2)^*\}$ can be found when maximizing the silicon activity.

Fig. 4 displays the present calculated two limits – precipitation of C or SiO_2 creation – which correspond to the "active oxidation window" of bare SiC surface in terms of silicon activity as a function of the inverse of temperature. We can see the solid–liquid reference change at the Si melting. This window shows that in the SiC existence domain only a certain SiC composition range bounded by C precipitation can support active oxidation. With increasing temperature pure silicon is produced at ≈2170 K for the condition of active oxidation. This Si(liq) can also be oxidized in active manner with SiO(g) evaporation or passive manner creating a SiO_2 layer. Note that – as shown in the same Fig. 4 the production of liquid silicon from the congruent interface SiO_2–SiC occurs at lower temperature, *i.e.* ≈1940 K. This domain is interesting for silicon production. In SiC manufacturing, this domain can be reached either using too high O_2 background pressure or with a remaining excess of SiO_2.

Fig. 5 displays the SiC "active oxidation window" in terms of surface (steady-state) oxygen pressure as a function of the

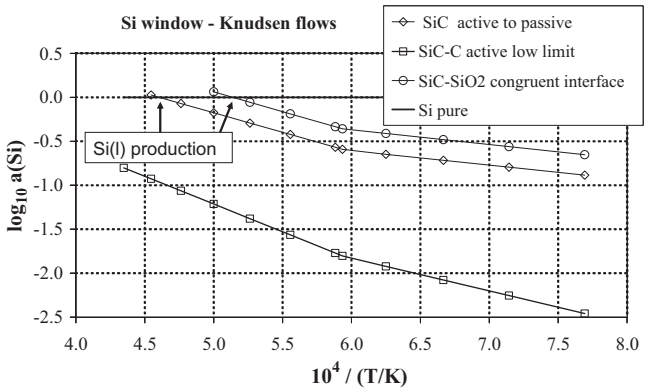

Fig. 4. Decimal logarithm of silicon activity limits for the active oxidation "window": (i) for active oxidation of SiC–C, *i.e.* at the limit of carbon precipitation, as a function of the inverse of temperature, (ii) for active to passive transition, *i.e.* creation of the first SiO_2 layer, and comparison to the silicon activity for congruent vaporization of the SiC–SiO_2 interface. Note the production of liquid silicon for different temperatures according to the state of the silica layer either as a congruent interface or at its transition from active to passive oxidation.

inverse of temperature. The high oxygen pressure limit is definitely different from the value for congruent vaporization. The oxygen partial pressure at SiC surface must be slightly higher than at the SiC/SiO_2 congruent interface because the supplementary condition imposed to the Si–C–O system is not the same: flow ratio or relation $p_{SiO}/p_{CO} = 3$ (or 3.76) for congruent vaporization meanwhile $p_{SiO}/p_{CO} = 1$ for active oxidation.

Concluding, the upper limit represents active to passive transition and is definitively different (i) from the interface condition for congruent vaporization of SiC–SiO_2 and (ii) and from the triphasic SiC–SiO_2–C. During de-oxidation of SiC with a silica layer – under the evolution toward non-oxidative conditions, *i.e.* neutral atmosphere or absolute vacuum – the oxygen pressure and silicon activity correspond to congruent vaporization of the SiC–SiO_2 interface and we obtain the passive to active transition. In the opposite, for a bare SiC surface submitted to increasing surface oxygen pressures (progressive external addition of

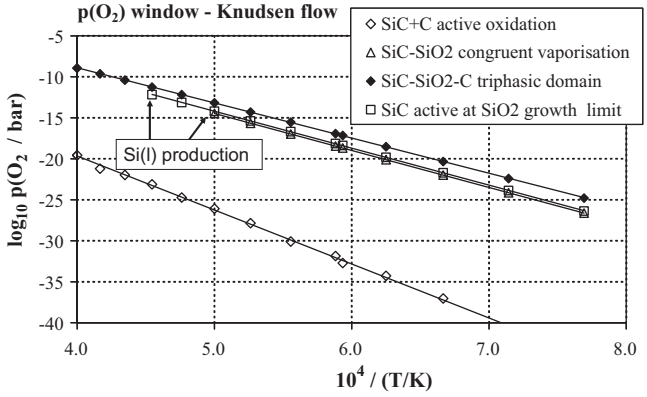

Fig. 5. Decimal logarithm of oxygen partial pressure limits for the active oxidation "window": (i) for active oxidation of SiC–C, *i.e.* at the limit of the carbon precipitation as a function of the inverse of temperature, (ii) for active to passive oxidation, *i.e.* creation of a first SiO_2 layer and comparison with the oxygen partial pressure for congruent reaction at the interface SiC–SiO_2 and for the triphasic SiC–SiO_2–C. All pressures are steady-state SiC surface pressures.

oxygen to SiC) this transition corresponds to the beginning of SiO_2 formation with slightly higher oxygen pressure and lower silicon activity. Independently of the experimental and characterization observations, the observed transition does correspond to an oxygen range values domain rather than to a fixed line when oxidizing or de-oxidizing. This range may be modified if some diffusion phenomena occur in the silica layer or bulk silicon carbide, the effect of which would be to modify the congruent oxygen potential at the interface SiC/SiO_2 for passive to active transition but not for the creation of the first silica layer (active to passive transition).

The silicon activity and oxygen pressure windows define the conditions for the existence of a bare or clean SiC surface. In the present work and for a better understanding, this window will be called "active oxidation window" although the carbon precipitate has been considered as part of the active range as usually presented in the literature.

3.2. SiC erosion under active oxidation

Contrarily to the vaporization of pure binary Si–C and ternary Si–C–O, the composition of the solid phase under active oxidation remains within the SiC non-stoichiometric composition domain when exposed to surface oxygen partial pressure values included in the window shown in Fig. 5 because the ratio of the atomic evaporation flow $F_{Si}/F_C = 1$. It vaporizes SiO(g), CO(g), Si(g), Si_2C(g), SiC_2(g), Si_2(g), Si_3(g), etc. with partial pressures as calculated from active oxidation conditions, *i.e.* for each couple {oxygen pressure, silicon activity} in the window as defined in Figs. 4 and 5. For the two limits of the active oxidation window, the *A* and *B* coefficients for decimal logarithmic plots of these partial pressures are displayed in Table 1. It was observed that even at the carbon rich limit the plots of partial pressures for species that include the Si atoms change their slopes for temperatures higher than the silicon melting temperature (1685 K) due to change of reference state for pure Si.

With the flows of Si and C coming from different gaseous species we calculated the SiC erosion – same definitions as in part I paper[12] – for each active oxidation limit as shown in Fig. 6.

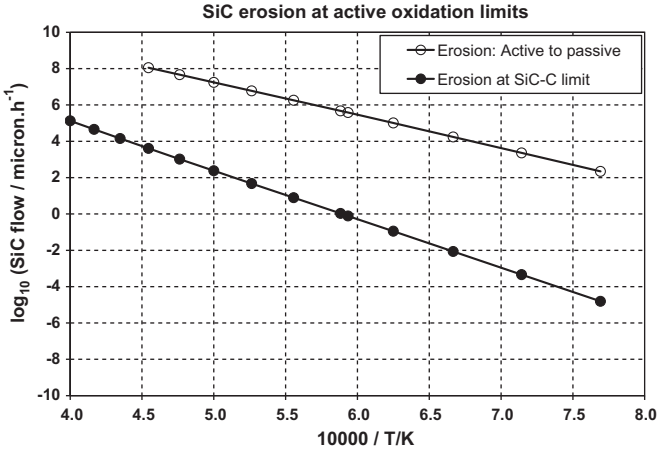

Fig. 6. SiC erosion flows (in $\mu m\,h^{-1}$) at the two limits of the active oxidation window of SiC.

As we can see the SiC looses are much more important (10^6 to 10^4 with temperature increase) close to the active to passive oxidation transition limit than near the carbon precipitation limit. More, the erosion rates at very high temperature appear very important – 10^4 μm (SiC limit) to about 10 m (active to passive limit) of SiC thickness per hour – and consequently non realistic because a so important gaseous quantity cannot be easily evacuated. For industrial processes, this means (i) that the SiC compound is very reactive to incident oxygen flow because SiO(g) and CO(g) are readily formed due to their intrinsic thermodynamic stability, (ii) the SiO(g) and CO(g) pressures can be very high notwithstanding the surface of SiC is provided with oxygen, (iii) and a rapid evolution toward the SiC–C limit is attended by depletion of oxygen in the incident gas flow as well as silicon activity decrease.

4. SiC re-deposition

Calculations of available deposition flows of Si and C are performed on the same basis as done in paper part I.[12] The reason for these calculations is to evaluate the impact of transport processes by the gas phase near equilibrium conditions, *i.e.* during condensation and evaporation on SiC inner surfaces of the porous samples. The transport process itself is slow and isothermal through out a large part of the sample and occurs in the SiC green materials during the oxygen departure since in the furnaces the walls are not totally closed and their material generally reacts with the vapors – nominally SiO(g) – meanwhile the CO(g) is partly coming back into the material from the furnace housing. Thus, small chemical gradients exists during the manufacturing process including curvature effects that exist also at the surface of grains as well as at their contacts.

4.1. Calculations of the available deposition flows

We calculated the evaporated Si and C atomic flows from the SiC and we obtained general erosion rates during any pure vaporization experiment in part I[12] or under active oxidation experiment in the previous Section 3. Some of these flows can condense on the surface of solid SiC to form new SiC crystals under the influence of any chemical potential local gradients. Even when assuming no gradient, the equilibrium conditions impose that condensation and evaporation flows are equal at any crystal surface when working in a quite close system as pores in a material. Assuming that the gaseous contained oxygen species CO(g) and SiO(g) do not recombine to form solid SiC according to the reverse of the main congruent vaporization reaction

$$3\,SiO(g) + CO(g) = 2\,SiO_2(s) + SiC(s) \quad (7)$$

since in active oxidation conditions there is no silica at the surface, only the Si and C flows from oxygen free gaseous species, such as Si(g), Si_2(g), Si_3(g), SiC_2(g), Si_2C(g), SiC(g), C(g) and C_3(g) are able to re-precipitated as SiC coming from vapor phase transport and reaction of silicon with carbon at any surface. It is equal to the carbon flow resulting from C contained species as Si_2C, SiC_2, SiC, C, C_3 which remains lower than the Si flow

Table 1
A and B coefficients for the decimal logarithmic plot of partial pressures according to $\log_{10}(p/\text{bar}) = A/(T/\text{K}) + B$ at the two limits of the active oxidation window of SiC. Note that with Si melting temperature at 1685 K the slopes change.

Active oxidation limit at	*A*		*B*	
SiC with SiO_2 creation (active to passive transition)	1000–1685 K	1685–2170 K[a]	1000–1685 K	1685–2170 K[a]
SiO(g)	−19082.4	−17375.5	9.11878	8.10791
CO(g)	−19082.4	−17861.4	9.02058	8.27924
CO_2(g)	−2.6872.1	−26372.0	8.63916	8.31896
SiO_2(g)	−31018.1	−30228.7	8.99839	8.52750
Si(g)	−24957.5	−24638.8	7.95240	7.77195
Si_2(g)	−33664.1	−33027.6	10.15628	9.79698
Si_3(g)	−37420.9	−36355.7	11.20982	10.60417
Si_2C(g)	−32688.8	−31857.3	10.35675	9.86816
SiC_2(g)	−37531.1	−36940.3	10.85326	10.48712
SiC(g)	−41219.4	−40713.7	10.35555	10.05202
C(g)	−39571.8	−39622.9	8.24849	8.26785
C_3(g)	−48026.1	−48179.4	10.56234	10.62042
Si activity in SiC	−1663.7	−4447.4	0.39373	2.04795
O_2(g)	−45483.4	−44932.2	8.61329	8.27373
O(g)	−36020.0	−35744.4	7.77219	7.60242
SiC with C precipitation	1000–1685 K	1685–2500 K	1000–1685 K	1685–2500 K
SiO(g)	−31398.9	−31103.0	8.15776	7.92872
CO(g)	−27274.4	−27365.5	8.03339	8.03705
CO_2(g)	−48075.1	−44851.4	8.70936	6.59535
SiO2(g)	−56351.2	−52935.1	9.09878	6.86899
Si(g)	−27019.8	−26752.3	7.96548	7.80445
Si_2(g)	−37788.7	−37254.6	10.18244	9.86198
Si_3(g)	−43607.8	−42696.2	11.24907	10.70167
Si_2C(g)	−34753.2	−33970.8	10.37140	9.90056
SiC_2(g)	−35465.4	−34826.8	10.83772	10.45442
SiC(g)	−41219.0	−40713.7	10.35525	10.05192
C(g)	−37506.6	−37509.4	8.23325	8.23525
C_3(g)	−41830.4	−41838.9	10.51662	10.52262
Si activity at SiC–C limit	−3726.0	−6316.3	0.40687	1.94477
O_2(g)	−66630.6	−6.6812.9	7.17499	7.18245
O(g)	−47654.1	−46040.8	7.81492	6.75691

[a] At this temperature silicon liquid begins to be produced from SiO_2–SiC mixtures under active oxidation (see Fig. 4).

whatever is the stoichiometric composition of SiC. This deposition flow is the minimum one attended. The C flow is calculated as explained in part I using for example the relation,

$$F_C = \frac{S}{\sqrt{2\pi RT}}\left[\frac{p_C}{\sqrt{M_C}} + \frac{3p_{C_3}}{\sqrt{M_{C_3}}} + \frac{p_{Si_2C}}{\sqrt{M_{Si_2C}}} + \frac{2p_{SiC_2}}{\sqrt{M_{SiC_2}}} + \frac{p_{SiC}}{\sqrt{M_{SiC}}}\right] \quad (8)$$

Furthermore, due to the Si flow in excess in the only Si–C gaseous phase – issued from Si(g), Si_2(g), Si_3(g) and any lack of atomic balance between Si_2C(g) and SiC_2(g) – different reactions can produce SiC(s) precipitation as for instance the main one,

$$2\,\text{Si(g)} + \text{CO(g)} = \text{SiC(s)} + \text{SiO(g)} \quad (9)$$

and following (by extension) half of the available Si-excess flow can be consumed for SiC deposition due to any CO(g) pressure in small excess as a background component of the carrier gas. The excess Si flow compared to C flow is calculated using the relation,

$$F_{Si} = \frac{S}{\sqrt{2\pi RT}}\left[\frac{p_{Si}}{\sqrt{M_{Si}}} + \frac{2p_{Si_2}}{\sqrt{M_{Si_2}}} + \frac{3p_{Si_3}}{\sqrt{M_{Si_3}}} + \frac{(2\text{-}1)p_{Si_2C}}{\sqrt{M_{Si_2C}}} + \frac{(1\text{-}2)p_{SiC_2}}{\sqrt{M_{SiC_2}}} + \frac{(1\text{-}1)p_{SiC}}{\sqrt{M_{SiC}}}\right] \quad (10)$$

in which the factors (2-1), (1-2) and (1-1) are used to take into account of the stoichiometric proportion of these molecules that has been already condensed with the minimum growth flow calculated on basis of the C flow.

Note that SiO(g) according to reaction (9) is produced detrimental to CO(g) and this effect tends to increase the SiO/CO ratio in the gas phase and to counterbalance the above needed excess of CO(g) and consequently the active oxidation conditions remains valid at the surface of SiC. The SiC resulting from this precipitation reaction added to SiC resulting from the only carbon gaseous flow is the maximum possible precipitation rate of SiC.

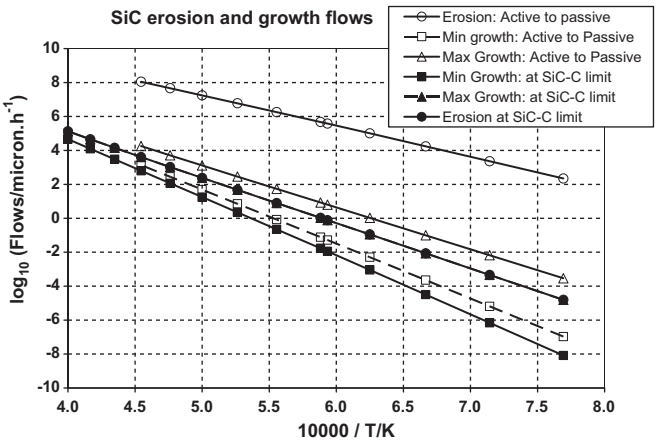

Fig. 7. Decimal logarithms of SiC minimum and maximum deposition rates during active oxidation at the limits of SiO_2 creation and C precipitation and comparison with the erosion flows by evaporation. All values are in μm of SiC per hour.

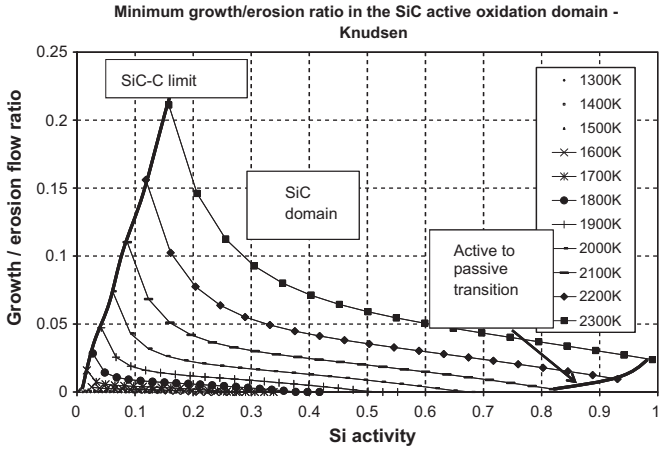

Fig. 8. Calculation of the minimum growth rate (see text) to erosion rate ratio for the active oxidation conditions of SiC as a function of the Si activity when the composition in the SiC non stoichiometric domain moves from the SiC–C limit to the active to passive transition (SiO_2 creation).

Fig. 7 displays the maximum and minimum possible SiC deposition flows for any SiC crystal under active oxidation with Si activity and oxygen pressures corresponding to the window limits as already defined. Comparing to the SiC erosion rate for the active oxidation window limits displayed in the same figure the possible SiC deposition rates are always lower than the SiC erosion rates whatever is the considered limit. This feature could be anticipated when looking at the partial pressures as quoted in Table 1: indeed, the partial pressures of SiO(g) and/or CO(g) are always higher than the main Si(g) pressure, except at the limit SiC–C for which Si(g) and CO(g) pressures become comparable.

The absolute values of available deposition rates appear very important at high temperature – between 10 μm and 1 mm per hour of SiC thickness at 2000 K – in relation with the vapor pressure of the different silicon gaseous species. Table 2 lists the obtained A and B coefficients of decimal logarithmic plots according to $\log(\text{Flows}) = A/T + B$ of the SiC erosion and minimum and maximum deposition rates for the different solid compositions of the active oxidation window limits.

Drawing the erosion rates and deposition rates for SiC under active oxidation in the same Fig. 7, we observe that: (i) the erosion rate at the limit of SiO_2 creation is far above all deposition rates, (ii) the erosion rate decreases largely when the SiC non stoichiometric composition moves toward the C precipitation limit, (iii) the deposition rates are always lower than the erosion rates in the active oxidation domain, and (iv) any efficient growth process by gas phase transport needs active oxidation conditions with a small available excess of CO(g) pressure in order to consume the excess of Si in the original gas phase produced by the SiC inner source material.

4.2. Influence of the non stoichiometric composition on the available growth rate

The above comparison of available growth rates with the erosion rates at the limit of the active oxidation window shows that the erosion rate increases strongly when going from the SiC–C limit to the active to passive transition (creation of a SiO_2(s) first layer at the surface of SiC) and consequently for increasing Si activities. The growth – minimum and maximum rates – to the erosion rates ratios are compared in Figs. 8 and 9, respectively, as a function of the Si activity in the active oxidation domain of SiC (the above defined window in Section 3.1).

We observe that the growth rate is maximum compared to the erosion rate for the limit SiC–C, and decreases rapidly when the composition of SiC goes toward the stoichiometric composition and the transition active to passive. The growth rate proportion increases markedly (up to 0.22) with temperature.

In Fig. 9, for the case of maximum growth with a slight available CO(g) excess, we observe a better ratio in favor of the growth which increases with temperature from 0.5 to 0.6 at the SiC–C limit. The influence of the composition when going toward the stoichiometric composition on the growth rate is less pronounced than for the minimum growth when compared to the maximum growth at the limit SiC–C, mainly at high temperature.

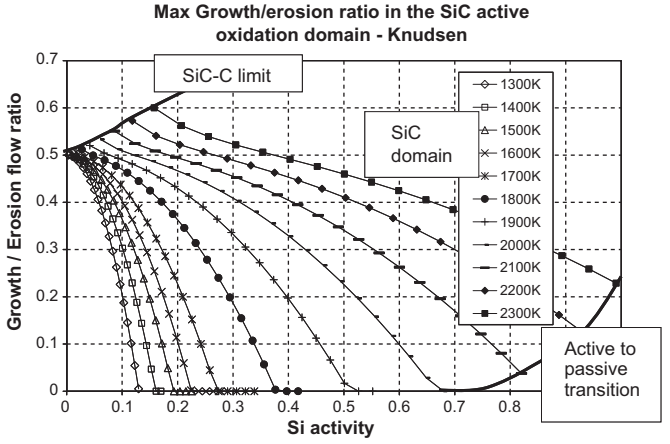

Fig. 9. Calculation of the maximum growth rate (see text) to erosion rate ratio for the active oxidation conditions of SiC as a function of the Si activity when the composition in the SiC non stoichiometric domain moves from the SiC–C limit to the active to passive transition (SiO_2 creation).

Table 2
Coefficients A, B for the decimal logarithmic plot of the possible SiC deposition rates under calculated oxygen pressure limits (and silicon activity limits) for active oxidation at C precipitation limit and at SiO_2 layer creation limit (active to passive limit) as a function of the inverse of temperature: $\log_{10} \Phi_d/(\mu m\, h^{-1}) = A/(T/K) + B$. Erosion rates are also mentioned at the limits of the active oxidation domain.

Active oxidation of SiC	Growth max is with small CO(g) excess (see text)	Coefficients		Coefficients	
		A	B	A	B
Temperature range		1000–1685 K[a]		1685–2170 K[a]	
SiO_2-limit (active to passive)	Growth max	−24,669	15.441	−24,731	15.476
	Growth min	−32,388	17.945	−31,777	17.578
	Erosion	−18,443	16.532	−17,775	16.132
Temperature range		1000–1685 K		1685–2500 K	
C-limit (active)	Growth max	−26,763	15.478	−27,250	15.751
	Growth min	−34,924	18.784	−34,192	18.344
	Erosion	−26,735	15.759	−26,816	15.797

[a] This limit corresponds to the production of liquid silicon with the active to passive transition.

4.3. SiC growth furnace conditions

Although the steady-state oxygen potential at the surface of SiC is very low under active oxidation conditions, the escaping flow associated with oxygenated species (SiO, CO, CO_2, etc.) is very large due to far higher pressures of these species. This means that the incident flow of oxygen must be very important to warranty steady state equilibrium conditions at the SiC surface to maintain a surface free from carbon and consequently the O_2(g) pressure in the furnace housings at room temperature (cold point) will be important to generate the needed incident oxygen flow. The incident flow of oxygen can be calculated if the gas flow regime between the furnace walls and the SiC surface is known.

Under vacuum, *i.e.* Knudsen conditions for $p \leq \approx 10^{-4}$ bar, the Knudsen relation can be used, and the following balance relation for the O atoms at the surface of SiC,

$$F_O^{inc} = \frac{2p_{O_2}^{furnace} C s_{wall}}{\sqrt{2\pi M_{O_2} RT^\circ}} = F_O^{evap} = \frac{C s_{SiC}}{\sqrt{2\pi RT}} \left[\frac{p_{SiO}}{\sqrt{M_{SiO}}} + \frac{p_{CO}}{\sqrt{M_{CO}}} + \frac{2p_{CO_2}}{\sqrt{M_{CO_2}}} + \frac{p_O}{\sqrt{M_O}} + \frac{2p_{O_2}}{\sqrt{M_{O_2}}} \cdots \right] \quad (11)$$

has been applied to determine the necessary O_2(g) pressure at the cold walls ($T^\circ = 300$ K) of the furnace to feed the SiC surface. C is the vacuum conductance between the SiC surface and the walls, taking into account on the thermal shields, and the surfaces s (walls and SiC) are taken as unity (the assumption is that SiC is strictly in front of a wall of the same surface). Note that in a furnace the ratio s_{wall}/s_{SiC} is normally slightly >1.

Under neutral gas viscous flow, the incident oxygen flow associated with the flow rate will be balanced close to the surface of SiC by the exhaust of SiO(g) and CO(g) species and a diffusion layer is created that decreases the exchange rates of all the species. In case of fast flows and no diffusion layer, with the assumption of surface equilibrium reactions, the above relation (11) can be applied for the only number of moles exchanged. This assumption represents the maximum rate of exchange available as already done by Nickel et al.,[11] and so calculated the oxygen pressure at the walls is an upper limit.

The two above regimes – Knudsen and viscous flow – are presented for the active to passive oxidation as well as to the C precipitation in Figs. 10 and 11. Table 3 gives the coefficients

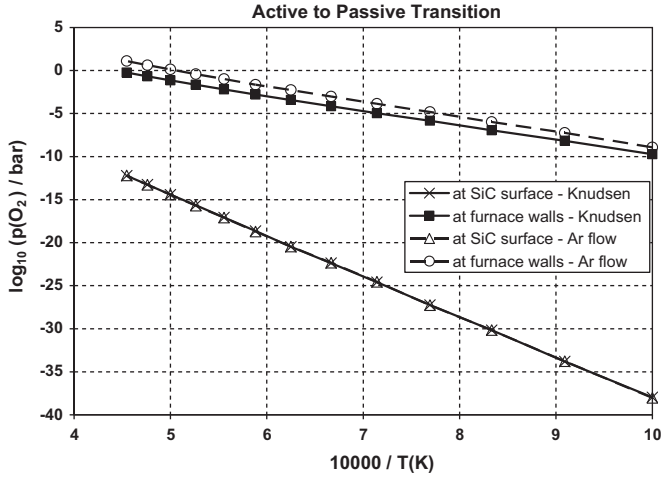

Fig. 10. Steady state of the di-oxygen pressures at the surface of SiC and at the wall furnace for the transition active to passive (creation of the first SiO_2 layer) and for two different flow regimes: vacuum (Knudsen flow) and under Ar (viscous flow).

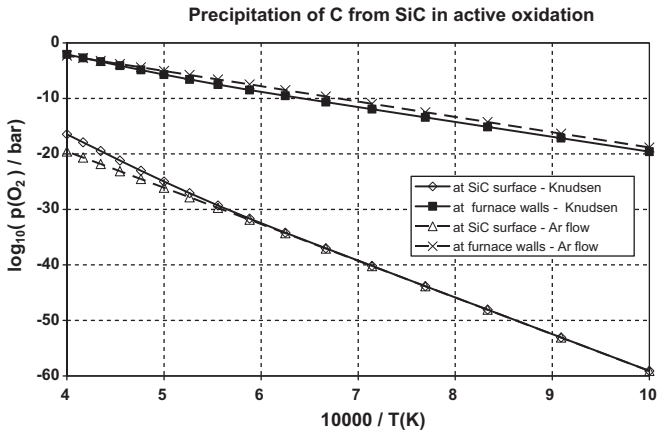

Fig. 11. Steady state of the di-oxygen pressures at the surface of SiC and at the wall furnace at the C precipitation limit under active oxidation and for two different flow regimes: vacuum (Knudsen flow) and under Ar (viscous flow).

Table 3
Coefficients of the oxygen pressure decimal logarithms $\log_{10} p(O_2/\text{bar}) = A/(T/\text{K}) + B$ for local partial pressures at the surface of SiC and at the furnace walls, and for two different flow regimes, vacuum (Knudsen) and pure Ar flow (viscous). N.B. The effect of a boundary diffusion layer in viscous flow at the surface of SiC is neglected. Conversely to Table 1 the fits of the pressures have been performed as a first approximation for the whole temperature range.

Local oxygen potential at	C precipitation (SiC–C limit) $1000 < T < 2500$ K		SiO_2 first layer (active to passive transition) $1000 < T < 2170$ K	
	A	*B*	*A*	*B*
SiC surface/Knudsen flow	−70,634	10.667	−47,166	9.1074
Furnace walls/Knudsen flow	−28,957	8.9394	−17,050	7.2776
SiC surface/Ar flow	−65,916	6.871	−47,159	9.1007
Furnace walls/Ar flow	−27,610	8.7618	−17,901	8.9645

for the decimal logarithms of the oxygen pressure at the surface of SiC and at the furnace walls. In Figs. 10 and 11 we observe that the oxygen pressure at the walls is effectively very high, and the Knudsen regime (referred to the wall furnace pressure of oxygen needed) which is an exact calculation of what happens under vacuum becomes readily not available for a SiC sample above temperatures of 1517 and 2290 K, respectively, for the creation of a first SiO_2 layer and for the C precipitation limit (total pressure $>10^{-4}$ bar). Figs. 10 and 11 show also that the manufacturing of SiC under active oxidation can support leaks of atmospheric pressure and high oxygen composition at the walls in the high temperature range.

We have to quote that exact flow calculations should be performed for high pressures, *i.e.* more that 10–100 mbar taking into account on diffusion in the gas flow regimes for the exact configurations of the furnaces.

5. Conclusion

The influence of oxygen on the vaporization behavior of SiC is presented for the so-called "active oxidation" conditions. We could see that if a certain steady-state oxygen pressure is imposed or more exactly is being the resulting of a flow exchange at the surface of SiC, the precipitation of SiO_2 or carbon at the surface of SiC can be prevented. The optimal SiC surface oxygen steady state partial pressure limits were calculated under which the homogeneous erosion of SiC would be achieved at different temperatures. We defined a double "window" in terms of oxygen partial pressures at the SiC surface in relation with silicon activity in the SiC compound for the so-called "active oxidation" of SiC. This kind of "window" becomes smaller at higher temperatures and the limit to the SiO_2 precipitation is close but definitely different from the oxygen partial pressure for the case of the so-called congruent vaporization of the SiC/SiO_2 interface or any triphasics $SiC–SiO_2–C$ or $Si–SiC–SiO_2$ as generally postulated by different authors in the literature.

The present calculated window of the oxygen partial pressure at the surface of SiC is related to a "clean" or bare SiC surface that must be an important condition for the SiC crystal growth. Calculations of the present window in terms of silicon activity show that only part of the non stoichiometric SiC composition domain can be reached according to these conditions, one border being the SiC–C composition limit. The fixed non stoichiometric composition for a fixed oxygen pressure will give specific electronic properties to the manufactured SiC compound – independently of any doping effects.

For the growth of SiC by deposition processes that may occur by vapor transport in the material itself – during sintering or mechanical consolidation by re-crystallization – the available SiC flows were calculated taking into account of either the only C contained gaseous species of the Si–C system or with the addition of a small excess of CO(g) provided by the background gas that allows the precipitation of the excess of silicon contained in the SiC vapor phase. The comparison between erosion flows and available growth flows showed that the growth or consolidation by deposition processes can occur only with the presence of CO(g) and is maximized for SiC compound compositions rich with carbon, *i.e.* close to the precipitation of carbon. However, the erosion flows are always larger than the available growth flows and this feature prevents the densification of pure SiC, *i.e.* under active oxidation conditions. The resulting grown SiC will be necessarily a SiC non stoichiometric compound rich with carbon and containing pores.

Fig. 12 summarizes, for isothermal conditions, the present analysis of the SiC oxidation and growth by enlarging intentionally the compositional domain of the non-stoichiometric SiC compound. Because the calculations were performed using the silicon activity as basic parameter we take it also as basic parameter for this summarizing figure. Beginning by silicon activity equal to 1, which corresponds to the silicon rich SiC compound, and following the diagonal line for activity decrease in the SiC non-stoichiometric domain toward the SiC–C limit, we arrive at the point of silicon activity for the congruent vaporization reaction of the $SiC–SiO_2$ pseudo-binary – *i.e.* congruent SiC/SiO_2 interface – built because of previous oxidation of SiC. The next point corresponds to the transition between active-to-passive oxidation, depending on the oxidation reaction – *i.e.* the first SiO_2 crystals or layer forming on a clean SiC surface submitted to an increasing oxygen impinging flow. In case of reduction – *i.e.* starting with an interface SiC/SiO_2 – it is the congruent point which operates for the disappearance of the last SiO_2 crystals. Then at decreasing silicon activity, we are in the domain where the surface of SiC is free of SiO_2, *i.e.* the domain of active oxidation. This area corresponds to a range of very low surface oxygen steady state pressures far lower than any oxygen pressure that can be deduced from volatility diagrams. The limit of low silicon activity and carbon apparition builds the end of this active oxidation domain associated with a pure SiC surface.

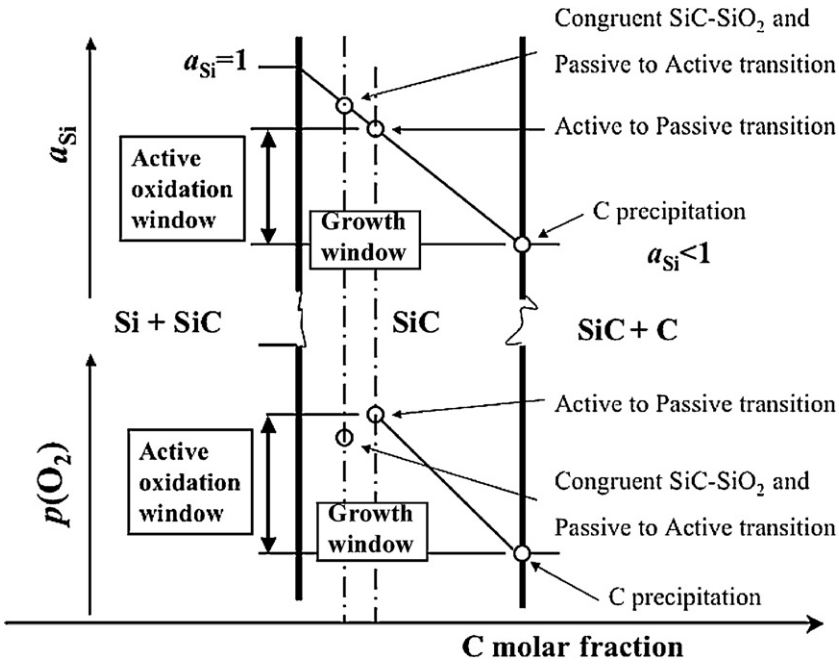

Fig. 12. Isothermal non stoichiometric composition domain of the SiC compound (intentionally enlarged) and SiC active oxidation composition range depending on the local surface steady state of the di-oxygen pressure and/or silicon activity as a result of our calculations. The available growth window is located in the active oxidation window close to the carbon precipitation limit.

The present calculations will help to explain some experimental results achieved while measuring the partial pressures in high temperature mass spectrometry and with a new reactor furnace fitted with capillary sampling mass spectrometer followed by characterizations of the links built between crystal powders after heat treatments.

Acknowledgment

The authors acknowledge St.-Gobain CREE research center at Cavaillon (France) for sponsoring the present study.

References

1. Vaughn WL, Mass HG. Active-to-passive transition in the oxidation of silicon carbide and silicon nitride in air. *J Am Ceram Soc* 1990;**73**:1540–3.
2. Hinze JW, Graham HC. The active oxidation of Si and SiC in the viscous gas-flow regime. *J Electrochem Soc* 1976;**123**:1066–73.
3. Narushima T, Goto T, Yokoyama Y, Igushi Y, Hirai T. High temperature active oxidation of chemically deposited silicon carbide in CO–CO_2 atmosphere. *J Am Ceram Soc* 1993;**76**:2521–4.
4. Opila EJ, Hann RE. Paralinear oxidation of CVD SiC in water vapor. *J Am Ceram Soc* 1996;**80**:197–205.
5. Schneider B, Guette A, Naslain R, Cataldi M, Costecalde A. A theoretical and experimental approach to the active-to-passive transition in the oxidation of silicon carbide. *J Mater Sci* 1998;**33**:535–47.
6. Rosner DE, Allendorf HD. High temperature kinetics of the oxidation and nitridation of pyrolytic silicon carbide in dissociated gases. *J Phys Chem* 1970;**74**:1829–39.
7. Balat M, Flamant G, Male G, Pichelin G. Active to passive transition in the oxidation of silicon carbide at high temperature and low pressure in molecular and atomic oxygen. *J Mater Sci* 1992;**27**: 697–703.
8. Wagner C. Passivity during the oxidation of silicon at elevated temperatures. *J Appl Phys* 1958;**29**:1295–7.
9. Opila EJ, Jacobson NS. *Oxidation and corrosion of ceramics in ceramics science and technology*. In: Chen I-W, Riedel R, editors. Germany: Wiley-VCH; in press.
10. Heuer AH, Lou VLK. Volatility diagrams for silica, silicon nitride, and silicon carbide and their application to high-temperature decomposition and oxidation. *J Am ceram Soc* 1990;**73**:2785–3128.
11. Nickel KG, Lukas HL, Petzow G. High temperature corrosion of SiC in hydrogen–oxygen environments. In: Hack K, editor. *The SGTE case book – thermodynamics at work*. Cambridge, UK: Woodhead Publishing Limited; 2008. p. 200–11.
12. Honstein G, Chatillon C, Baillet F. Thermodynamic approach to the vaporization and growth phenomena of SiC ceramics. I. SiC and SiC–SiO_2 mixtures under neutral conditions, *J Eur Ceram Soc*; in press, doi:10.1016/j.jeurceramsoc.2011.11.032.
13. Rocabois P, Chatillon C, Bernard C. High temperature analysis of the thermal degradation of silicon-based materials. II: ternary Si–C–O, Si–N–O and Si–C–N compounds. *High Temp High Press* 1999;**31**, 433-454.